

UFO: A unified method for controlling Understandability and Faithfulness Objectives in concept-based explanations for CNNs

Vikram V. Ramaswamy, Sunnie S. Y. Kim, Ruth Fong, Olga Russakovsky
Princeton University

{vr23, suhk, ruthfong, olgarus}@cs.princeton.edu

Abstract

Concept-based explanations for convolutional neural networks (CNNs) aim to explain model behavior and outputs using a pre-defined set of semantic concepts (e.g., the model recognizes scene class “bedroom” based on the presence of concepts “bed” and “pillow”). However, they often do not faithfully (i.e., accurately) characterize the model’s behavior and can be too complex for people to understand. Further, little is known about how faithful and understandable different explanation methods are, and how to control these two properties. In this work, we propose UFO, a unified method for controlling Understandability and Faithfulness Objectives in concept-based explanations. UFO formalizes understandability and faithfulness as mathematical objectives and unifies most existing concept-based explanations methods for CNNs. Using UFO, we systematically investigate how explanations change as we turn the knobs of faithfulness and understandability. Our experiments demonstrate a faithfulness-vs-understandability tradeoff: increasing understandability reduces faithfulness. We also provide insights into the “disagreement problem” in explainable machine learning, by analyzing when and how concept-based explanations disagree with each other.

1. Introduction

As convolutional neural networks (CNNs) start to be used to make consequential decisions, such as those in medical diagnosis and treatment, there is a need for these models to be interpretable. Over the past decade, many model explanation methods have been proposed, ranging from local methods that explain a single prediction, e.g., by highlighting relevant pixels in an input image [5, 7, 19, 23, 24, 27, 28, 29], to global methods that provide a higher-level understanding of what the model has learned and how it predicts a certain target class [4, 8, 22, 31]. However, explanations often disagree with each other [17], making it difficult for users to choose which explanation method to use.

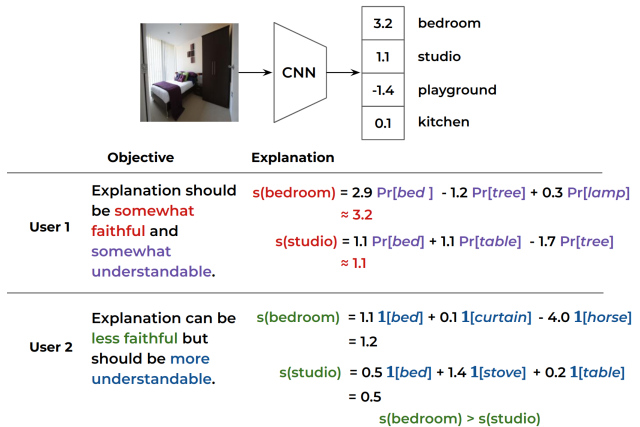


Figure 1. Consider a CNN that outputs probabilities for the target classes (e.g., bedroom, studio). For explanations, different users might have different objectives of (1) “faithfulness”: matching probabilities of target classes (user 1, “somewhat faithful”) vs. just matching the output class (user 2, “less faithful”) and (2) “understandability”: encoding concepts as probabilities (user 1, “somewhat understandable”) or binary values (user 2, “more understandable”). Our proposed method unifies existing concept-based explanation methods for CNNs and enables users to control “faithfulness” and “understandability.”

One reason for this disagreement is the lack of consensus among researchers about the goals of these methods. While most methods attempt to optimize objectives like “faithfulness” and “understandability,” these terms are not well defined and can be translated into different mathematical objectives. For example, “faithfulness” requires that the explanation accurately describes the model’s behaviour, but this can be thought of at different levels: Do we care about the distribution of all class scores from the model (as in [31, 16])? Or just the score for the target class (as in [22])? Similarly, “understandability” can mean different things to different explanation users: AI experts (e.g., model developers) may find an explanation that encodes concepts as probabilities understandable, while non-experts (e.g., lay end-users) may not and thus, prefer an explanation that en-

codes concepts as binary values [14]. In Fig. 1, we show how different users might want different levels of faithfulness and understandability in model explanations.

In this work, we propose UFO, a novel concept-based CNN explanation method that formalizes (U)nderstandability and (F)aithfulness as mathematical (O)bjectives. UFO unifies existing methods [4, 8, 12, 16, 31] that provide an explanation for an output of a CNN model layer in terms of pre-defined semantic concepts. However, different from these works, UFO enables users to explicitly set the desired levels of faithfulness and understandability, and seamlessly obtain an explanation that is suitable for their needs.

Our main contributions are as follows:

- We operationalize the notions of “faithfulness” and “understandability” and propose a set of definitions for each of these terms. We then integrate them into a unified concept-based explanation method which is flexible enough to accommodate the different notions depending on the downstream application.
- We demonstrate how the method can be used to generate explanations of varying levels of faithfulness and understandability, and analyze where these explanations differ. This reveals a number of insights into how concept are selected by concept-based explanations, and which concepts are more likely to be used to explain a model. We demonstrate how frequency, size, and learnability of the selected concepts differ across the different explanation objectives.
- We discuss how our method generalizes and unifies most prior concept-based explanation approaches. We empirically validate this assertion by comparing our produced explanations to those from 3 prior works (NetDissect [4], IBD [31] and ELUDE [22]).

UFO enables researchers and practitioners to reason concretely about choices for understandability and faithfulness, and compare to methods with similar incentives.

2. Related work

Concept-based explanation methods are a popular class of model explanation methods that explain model behaviour and outputs with human-understandable semantic concepts. They can be categorized along several axes. First, there are methods that explain some aspect of a model post-hoc [4, 8, 12, 22, 31]. NetDissect [4] and Net2Vec [8] give insights about what the model has learned by identifying which neuron or which set of neurons encode a specific concept. On the other hand, TCAV (Testing with Concept Activation Vectors) [12] learns vectors in the model activation space that corresponds to concepts and use them to quantify

how sensitive the model’s predictions are to a specific concept. Other methods focus on explaining how a model predicts a certain target class [22, 31]. IBD (Interpretable Basis Decomposition) [31] first learns concept vectors in the model activation space, then decomposes the model’s prediction in terms of these vectors. ELUDE (Explanation via Labelled and Unlabelled DEcomposition) [22] also decomposes the model’s prediction, but focuses on characterizing what portion of the prediction can and cannot be explained with available concepts.

More recently, concept-based “interpretable-by-design” models have been proposed [16, 18, 20, 6]. They all take the concept bottleneck approach where the full model consists of a bottleneck that recognizes concepts in an input image and a discriminative model that classifies the image based on the bottleneck outputs (concept scores). The discriminative model is parameterized as an interpretable model (e.g., linear model, generalized additive model), which makes the full model interpretable, i.e., an interpretable discriminative model reasoning with interpretable features (concepts recognized by the bottleneck). The differences between each work lie in their choice of parameterization and training algorithm for the bottleneck and the discriminative model.

Although all these methods are called “concept-based,” the relationship between them are largely unclear. This poses a huge challenge to researchers and practitioners who want to compare different methods’ capabilities, constraints, and (implicit) assumptions. In this work, we address this challenge by presenting a unified method that encapsulates and characterizes all aforementioned methods with respect to two axes: faithfulness and understandability.

Our work is similar in spirit to a growing body of works that introduce analyses and frameworks to better understand, evaluate, and compare model explanation methods [1, 2, 3, 9, 13, 21, 25]. In particular, Han et al. [9] also argue the need for a unified framework and propose one for attribution heatmap explanations (specifically perturbation and gradient-based methods), which aim to explain which input features are relevant to a model’s output decision. Ramaswamy et al. [21] examine concept-based methods as we do, but they focus on analyzing commonly overlooked factors: probe dataset choice, concept learnability, and number of concepts used in an explanation. On the other hand, we introduce a unified method (UFO) that deepens our understanding of the behavior of concept-based methods and their relation to one another.

UFO also enables researchers and practitioners to generate customized explanations by turning the knobs of faithfulness and understandability.

3. UFO: A unified method for generating concept-based explanations for CNNs

We now propose our unified method (Understandability and Faithfulness Operationalization) for concept-based explanations, which explain some aspect of the model’s output (either its final prediction or intermediate scores) in terms of a set of pre-defined semantic concepts. We develop this as a post-hoc explanation method: generating an explanation when given access to the trained model as well as a *probe dataset*, a dataset similar to the training dataset that is labelled with a set of concepts.

Given. Concretely, consider an image classification CNN model $F: \mathcal{X} \rightarrow \mathbb{R}^D$, which outputs a vector of dimension D when given an image $x \in \mathcal{X}$ as an input, and let $y(x) = \arg \max F(x)$, which outputs a model’s prediction. Note that F here may be the final or an intermediate layer output of the model, corresponding to the layer we aim to explain.¹

We want to explain this output in terms of C semantic concepts. To do so, we use a probe dataset $X \subset \mathcal{X}$, where each $x \in X$ is annotated $A(x) \in \{0, 1\}^C$ with the presence or absence of each of these concepts. By correlating the presence or absence of these concepts with the model’s output, we can identify what human-understandable concepts are contributing to the model’s predictions.

Explanation framework. We consider $F = g \circ f$ as a combination of an intermediate function $f: \mathcal{X} \rightarrow \mathbb{R}^n$, which produces a set of n image features (that we will attempt to explain using the C concepts), and a function $g: \mathbb{R}^n \rightarrow \mathbb{R}^D$, which combines the features into the D -dimensional output.

We explain F by learning two functions $h_{\text{conc}}: \mathbb{R}^n \rightarrow \mathbb{R}^C$, which maps the features f to the concepts, and a function $h_{\text{pred}}: \mathbb{R}^C \rightarrow \mathbb{R}^D$, which maps the concepts to the model output F . Then, we have two different objectives:

1. To maximize the **faithfulness** of the explanation. Simply put, this objective requires the explanation to mimic the model’s output as far as possible, i.e., $F(x) \approx h_{\text{pred}} \circ h_{\text{conc}} \circ f(x)$.
2. To maximize the **understandability** of the explanation. An explanation that perfectly mimics the model but is not human-understandable doesn’t make the model more interpretable: humans need to be able to parse the explanation resulting from h_{pred} and h_{conc} .

Currently, there is no clear consensus on what these two different terms could mean. In the following subsections, we explore the definitions that each of these objectives could take and highlight how our proposed definitions can describe existing concept-based explanations.

¹If F is the final layer of the model, we will demonstrate in Sec. 3.3 that our framework can be adapted to explain the model’s predicted class $y(x) = \arg \max F(x)$ instead of the model’s full output.

3.1. Faithfulness

We can vary the faithfulness of an explanation by changing the definition for how an explanation should mimic a model’s output (i.e., how an explanation of the form $h_{\text{pred}} \circ h_{\text{conc}}$ approximates g , the latter part of a model). We describe three definitions below:

1. **Most faithful (FFF).** First, we can match the full D -dimensional output of our explanation with that of the model for all possible images, not just those in the probe dataset (i.e., \mathcal{X} instead of X). One way to achieve this would be to learn h_{conc} and h_{pred} such that $h_{\text{pred}} \circ h_{\text{conc}} = g$.
2. **Somewhat faithful (FF).** Next, we can relax our first definition and require that the full outputs of the explanation and model match only for images in the probe dataset. Then, rather than requiring $h_{\text{pred}} \circ h_{\text{conc}} = g$, we would minimize the following mean-squared error (MSE) loss for all $x \in X$:

$$\|g \circ f(x) - h_{\text{pred}} \circ h_{\text{conc}} \circ f(x)\|. \quad (1)$$

This would be potentially more useful to developers who wish to debug or improve a model: explanations that model the full score distribution allow for better diagnoses of the model.

3. **Least faithful (F).** Finally, instead of mimicking the model’s full output, our explanation can mimic just the model’s prediction. Then, we would minimize the following cross-entropy (CE) loss for all $x \in X$:

$$CE(y(x), h_{\text{pred}} \circ h_{\text{conc}}). \quad (2)$$

This would be more useful for end-users of the model, who just want to understand how a specific prediction is being made.

3.2. Understandability

The understandability of an explanation can vary along the following three axes:

Complexity of functions. The choice of the two learned explanation functions h_{conc} and h_{pred} can vary the understandability of the explanation. These can be general functions; however, they are typically chosen as linear functions in most concept-based explanation methods. A linear h_{conc} makes it easy to learn h_{conc} , while a linear h_{pred} makes it easy for a human to understand a model’s prediction as a linear combination of concepts.

Number of concepts. Prior works have shown that humans can realistically only reason with a small number of K concepts (typically with $K = 16$ or 32) [21]. Thus, we allow the user to select K concepts using a selection matrix S that

picks K out of C concepts and let $\mathbb{1}_S$ be the indicator vector of these K chosen concepts. Then, we can describe our explanation as $h_{\text{pred}} \circ \mathbb{1}_S \circ h_{\text{conc}} \circ f(x)$.

Concept encoding. Humans can more easily reason with binary values for concepts (e.g., is a bed present or absent?) than they can with continuous values for concepts (e.g., the probability of bed being present is 0.74). Thus, we can describe how concepts are encoded as binary values (**UUU**), probabilities (**UU**), or continuous values (**U**). When given a concept encoding $u \in \mathcal{C}$, we define \mathcal{C} as follows:

1. **Most understandable (UUU).** $\mathcal{C} = \{0, 1\}^C$.
2. **Somewhat understandable (UU).** $\mathcal{C} = [0, 1]^C$.
3. **Least understandable (U).** $\mathcal{C} = \mathbb{R}^C$.

In our main experiments, we use linear functions for h_{conc} and h_{pred} , set $K = 16$ concepts, and vary understandability based on how concepts are encoded.

3.3. Operationalization of explanations

Now, we instantiate specific objective functions using our different definitions of faithfulness and understandability. Our objective functions are all of the following form, where we find the optimal selection matrix S that chooses K semantic concepts, and the optimal functions h_{conc} mapping the features f to the C semantic concepts and h_{pred} mapping these concepts to the model predictions:

$$\arg \min_{h_{\text{conc}}, h_{\text{pred}}, S} \lambda_1 L_{\text{mimic}} + \lambda_2 L_{\text{align}} \quad (3)$$

Here, L_{mimic} varies based on the specific definitions used and describes how an explanation should mimic a model, while L_{align} is fixed as follows and describes how h_{conc} aligns features to concepts for images in the probe dataset:

$$L_{\text{align}} = \sum_{x \in \mathcal{X}} \sum_i CE(\mathbb{1}_S \circ h_{\text{conc}} \circ f(x)_i, \mathbb{1}_S \circ A_i(x)) \quad (4)$$

Then, hyperparameters λ_1 and λ_2 allow us to prioritize the mapping from the features to the concepts over the mapping from the concepts to the final output, and vice-versa.

We start with the simplest definition of L_{mimic} .

Least understandable, most faithful (U, FFF):

$$L_{\text{mimic}}^{\text{U, FFF}} = \sum_{x \in \mathcal{X}} \|g \circ f(x) - h_{\text{pred}} \circ \mathbb{1}_S \circ h_{\text{conc}} \circ f(x)\| \quad (5)$$

However, decomposing a general g into h_{conc} and h_{pred} is not tractable, as this would require us to minimize the above for all images $x \in \mathcal{X}$ (not just those in the probe dataset X).

Instead, we consider only losses that are tractable by using less strict definitions of faithfulness below.²

²Changes to the previous equation are denoted in **bolded red**.

Least understandable, somewhat faithful (U, FF):

$$L_{\text{mimic}}^{\text{U, FF}} = \sum_{x \in X} \|g \circ f(x) - h_{\text{pred}} \circ \mathbb{1}_S \circ h_{\text{conc}} \circ f(x)\| \quad (6)$$

Here, we are only concerned mimicking full outputs on the probe dataset and thus have a tractable objective.

Eq. (6) can also be modified to be more understandable. Rather than using the continuous output of $h_{\text{conc}} \circ f(x)$, we could also use a probabilistic version of it.

Somewhat understandable, somewhat faithful (UU, FF):

$$L_{\text{mimic}}^{\text{UU, FF}} = \sum_{x \in X} \|g \circ f(x) - h_{\text{pred}} \circ \mathbb{1}_S \circ p \circ h_{\text{conc}} \circ f(x)\| \quad (7)$$

where $p: \mathbb{R}^n \rightarrow [0, 1]^C$ is a function that maps features to probabilities (e.g. the sigmoid function).

We can make the explanation even more understandable by replacing $p \circ h_{\text{conc}} \circ f(x)$ entirely with the binary, ground-truth attributes encoded by $A(\cdot)$, i.e., explaining the model's output with perfect knowledge of the concepts.

Most understandable, somewhat faithful (UUU, FF):

$$L_{\text{mimic}}^{\text{UUU, FF}} = \sum_{x \in X} \|g \circ f(x) - h_{\text{pred}} \circ \mathbb{1}_S \circ \mathbf{A}(x)\| \quad (8)$$

Finally, we could use the least strict definition of faithfulness, where we only care about mimicking the single model prediction $y(x)$ rather than its full output $g \circ f(x)$. This can be paired with all three understandability definitions.

Least understandable, least faithful (U, F):³

$$L_{\text{mimic}}^{\text{U, F}} = \sum_{x \in X} CE(y(x), h_{\text{pred}} \circ \mathbb{1}_S \circ h_{\text{conc}} \circ f(x)) \quad (9)$$

Somewhat understandable, Least faithful (UU, F):

$$L_{\text{mimic}}^{\text{UU, F}} = \sum_{x \in X} CE(y(x), h_{\text{pred}} \circ \mathbb{1}_S \circ p \circ h_{\text{conc}} \circ f(x)) \quad (10)$$

Most understandable, least faithful (UUU, F):

$$L_{\text{mimic}}^{\text{UUU, F}} = \sum_{x \in X} CE(y(x), h_{\text{pred}} \circ \mathbb{1}_S \circ \mathbf{A}(x)) \quad (11)$$

3.4. Optimization

The trickiest part of the optimization is the selection of K concepts out of C concepts in total, since this is non-differentiable. Based on prior work, we assume h_{pred} and h_{conc} to be linear functions, and use a group Lasso regularization [26] that forces the squared sum of the coefficients of a concept to 0. That is, h_{pred} is learned as a coefficient matrix $W_{\text{pred}} \in \mathbb{R}^{D \times C}$. Assuming that the columns of

³Changes to $L_{\text{mimic}}^{\text{U, FF}}$ given by Eq. (6) are denoted in **bolded blue**.

	Binary		Grouped		Fine-grained	
	FF	F	FF	F	FF	F
UUU	4.20	7.13	2.95	12.59	4.12	60.43
UU	6.79	5.00	2.54	7.81	3.39	41.26
U	0.93	15.08	1.26	9.81	2.20	23.80

Table 1. **Gap between explanation and model outputs (Sec. 4.1.1).** For three Places365 models (binary, grouped, and fine-grained), we report the mean L2 distance between the distributions output by the explanation and the model (\downarrow is better) when varying levels of faithfulness and understandability. For each model, we **bold** the most faithful explanation, i.e., explanation with the lowest mean L2 distance. As expected, somewhat faithful (**FF**) explanations have lower mean L2 distance than least faithful (**F**) explanations. Also as expected, least understandable (**U**) explanations have lower mean L2 distance than somewhat understandable (**UU**) and most understandable (**UUU**) explanations, demonstrating a faithfulness-vs-understandability tradeoff.

W_{pred} are sorted in increasing order of their squared ℓ_2 norm ($\sum_{j=1}^D (W_{\text{pred}})_{j,i}^2$) (i.e. 1st column has smallest ℓ_2 norm, followed by 2nd column, etc.), during training, we add the following regularization loss:

$$L_{\text{reg}} = \sum_{i=1}^{C-K} \left| \sum_{j=1}^D (W_{\text{pred}})_{j,i}^2 \right| \quad (12)$$

We gradually increase the weight of this loss during training, initially allowing the W_{pred} to use all concepts to identify the most relevant ones, and then forcing the $C - K$ smallest columns of W_{pred} to 0.

4. Experiments

In Sec. 4.1, we analyze the faithfulness-vs-understandability tradeoff by optimizing Eqs. (6) to (11) for the same model and examine which concepts are highlighted in each case. We find that an explanation’s accuracy decreases as the explanation is made more understandable and that the concepts highlighted are highly dependent on the equation optimized. In Sec. 4.2, we compare our results to that of prior works [4, 31, 22].

4.1. Faithfulness-vs-understandability tradeoff

Experimental setup. We use a ResNet18 [10] model trained on Places365 [30] as our blackbox model to explain. This model takes as input an image and outputs a vector with the predicted probabilities of the image belonging to each of the 365 classes. Similar to ELUDE [22], we consider these predictions at 3 different granularities (using annotations provided in the dataset):

1. **Binary** (2 classes): “indoor” vs. “outdoor” scenes
2. **Grouped** (16 classes): coarse-grain scene categories (e.g., “home/hotel” or “forest/field/jungle”)

3. **Fine-grained** (365 classes): scene labels (e.g., “bedroom” or “bamboo forest”)

For binary and grouped scene predictions, we replace and retrain the final layer of the model. For fine-grained predictions, we analyze the 365-class model but focus only on explaining the top 20 classes that are most represented within the probe dataset, to simplify computation.

We use the ADE20k [32, 33] dataset (license: BSD 3-Clause) as the probe dataset with which to generate explanations, splitting its images randomly into train (60%, 11839 images), val (20%, 3947 images), and test (20%, 3947 images). We use train to optimize Eqs. (6) to (11), val to pick hyperparameters (e.g., λ_1, λ_2), and test to measure the accuracy of the explanation (i.e., the number of images for which the discrete explanation output matches that of the model). In [4], this dataset was further densely labelled with 1197 concepts comprising of objects, object parts, scenes, colors and textures; we use a subset of these concepts. First, we remove concepts that occur in fewer than 20 images within the training dataset. This gives us a set of 309 concepts. We further prune these concepts to remove concepts that are correlated with each other, following the findings of [21]. Correlations between concepts can be computed using the ground truth scores or the learned score of the concept. Surprisingly, we find that these result in very different correlations. Thus, we select the set of concepts separately for each setting of understandability (**UUU**, **UU**, **U**). More details are given in the appendix.

We use linear models for h_{conc} and h_{pred} , with $f(x)$ as the output of the penultimate layer of the model. These are trained for 5000 epochs with batch size = 1024 using either cross entropy or MSE loss (F vs. FF) and the Adam [15] optimizer with a learning rate = 1e-3. We set λ_1 and λ_2 as hyperparameters by picking the ratio $\lambda_1 : \lambda_2$ that has the highest validation accuracy. Finally, we set the number of concepts used to $K = 16$ (for the binary classifier) or $K = 32$ (for the grouped and fine-grained classifiers) concepts, based on prior work [21]. See the supp. mat. for details.

4.1.1 How well do explanations emulate the model?

We first analyze how well different explanations emulate the model as we vary the levels of faithfulness and understandability. We do so by measuring and comparing the average L2 distance between the distributions output by the explanation and the model, which capture how well the explanation emulate the model. See Tab. 1 for the full results. We find that, as expected, the L2 distance is lower for the somewhat faithful (**FF**) explanation, as compared to the least faithful (**F**) explanation. Moreover, we find that as the understandability increases, the faithfulness decreases: the least understandable (**U**) explanation emulates the model better than the somewhat understandable (**UU**) and the most un-

		most understandable UUU	somewhat understandable UU	least understandable U
bedroom	FF	bed, <i>building</i> , pillow	<i>bulletin board</i> , counter , <i>footbridge</i>	wardrobe , <i>pitcher</i> , <i>flag</i>
	F	<i>cap</i> , <i>buffet</i> , <i>saucepan</i>	counter , <i>food</i> , <i>refrigerator</i>	clock, lamp, wardrobe
conference-room	FF	bed , table , <i>building</i>	loudspeaker, <i>faucet</i> , table tennis	double door, table , desk
	F	bed , <i>rack</i> , <i>cup</i>	<i>tree</i> , <i>earth</i> , <i>sink</i>	table , crt screen, plant
crosswalk	FF	road, <i>building</i> , person	backpack , land , <i>cap</i>	backpack , <i>paper</i> , flag
	F	<i>step</i> , <i>floor</i> , <i>platform</i>	<i>bush</i> , land , <i>loudspeaker</i>	backpack , poster, <i>mountain</i>
downtown	FF	<i>building</i> , wall , sky	telephone booth, footbridge, backpack	baby buggy, flag , <i>ladder</i>
	F	<i>rack</i> , <i>step</i> , <i>platform</i>	<i>bush</i> , <i>seat</i> , <i>loudspeaker</i>	flag , <i>door</i> , wall
kitchen	FF	work surface, bed , <i>building</i>	<i>grandstand</i> , <i>backpack</i> , faucet	<i>pitcher</i> , crt screen, faucet
	F	bed , <i>loudspeaker</i> , <i>post</i>	<i>loudspeaker</i> , <i>sand</i> , refrigerator	cabinet, refrigerator , windowpane

Table 2. **Selected concepts vary based on faithfulness-understandability setting.** We compare the concepts selected to explain the fine-grained scene model under the six faithfulness-understandability settings ($\{\text{UUU}, \text{UU}, \text{U}\} \times \{\text{FF}, \text{F}\}$). We focus on a subset of randomly-selected scenes. For each, we highlight the top 3 concepts (i.e., highest absolute coefficients of h_{pred}). *Red* denotes a concept with a negative coefficient, *blue* denotes one with a positive coefficient, and **bold** emphasize a concept that is a top-3 concept for at least two of the six explanations for a given scene. We find that the concepts highlighted differ wildly across different definitions of faithfulness and understandability.

derstandable (UUU) explanations. This suggests a trade-off between faithfulness and interpretability: explanations that emulate the model well can be less understandable. Applications that require precise mimicking of the model’s predictions (for example, if being used to debug a model) would be better explained using the less understandable, more faithful (U, FF) version of UFO, whereas explanations being given to a lay-person might require higher understandability and thus, be better explained using a more understandable, less faithful (UUU, F) version of UFO.

4.1.2 How do “important” concepts change?

Next we analyze how “important” concepts, i.e., concepts selected by the explanation, change as we vary the faithfulness and understandability objectives. We find that the important concepts are very different under different objectives: Table 2 shows the three most important concepts (i.e., the three concepts with the highest absolute coefficients in h_{pred}) for a subset of coarse-grained scene groups.

We notice there are significant differences between the selected concepts under different settings of faithfulness and understandability. For example, consider the most understandable explanation setting. When using the somewhat faithful (FF) setting, the top 3 concepts for the scene “bedroom” include “bed,” “building” and “pillow” (with a negative coefficient for “building”). For the least faithful (F)

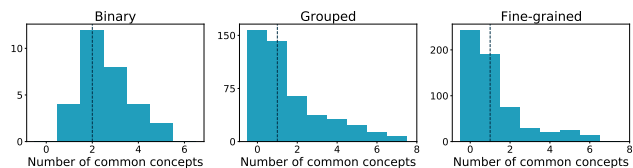


Figure 2. **Concept overlap (Sec. 4.1.2).** For three Places365 models (binary, grouped, and fine-grained), we report the number of shared concepts selected by the six different types of explanations ($\{\text{UUU}, \text{UU}, \text{U}\} \times \{\text{FF}, \text{F}\}$). Concretely, for each scene class, we identify the 10 most important concepts (based on the absolute coefficient value) for each type of explanation, and measure the overlap in concepts between each pair of explanations. We see that the average overlap is extremely low, between 1 and 2 concepts for most classes, indicating that the selection of the right understandability and faithfulness objectives is critical.

setting, the top 3 concepts are instead “cap”, “buffet”, and “saucepan.” In order to quantify this better, we consider the overlap among the top 10 concepts for each class. We see that the median overlap is just 1 for fine-grained scenes and grouped scenes, and 2 for binary (Fig. 2).

Given that the concept overlap is so low, we analyze what concepts are chosen by different types of explanations. We consider different aspects of the concepts chosen: the frequency (fraction of images that contain the concept), the average size (fraction of the image occupied by the segmen-

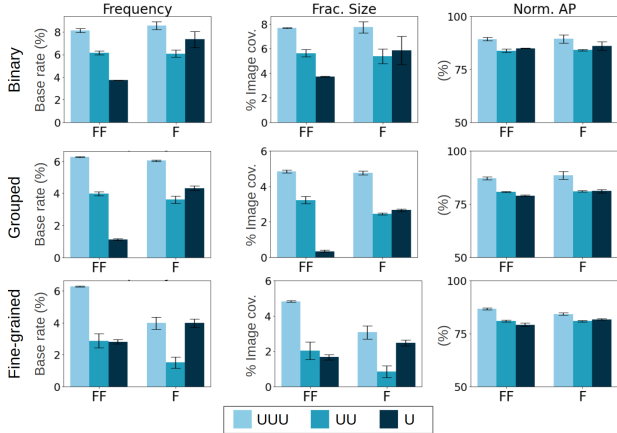


Figure 3. **Comparison of concepts chosen.** We compare the concepts based on their *frequency*, the average *size* of the concept within an image (fraction size) and the *learnability* of the concept from the feature space (normalized AP), across the 6 ($\{\text{UUU}, \text{UU}, \text{U}\} \times \{\text{FF}, \text{F}\}$) settings. In general, we see that concepts chosen by the **UUU** setting are typically larger, occur more often and are easier to learn, compared to the **UU** and **U** settings.

tation mask of the concept), and the learnability (measured using the normalized average precision and the ROC AUC). In general, we find that concepts highlighted by the most understandable (**UUU**) explanation tend to occur more often, be larger in size, and be more learnable, as shown in Fig. 3. For somewhat faithful explanations (**FF**), we see that for all metrics, somewhat understandable (**UU**) explanations contain more frequently occurring, larger and easier to learn concepts than less understandable (**U**) explanations. However, for less faithful (**F**) explanations, this trend does not always hold. We interpret this as follows.

For the **UUU** formulation, the *frequency* of the concept occurrence is directly related to the amount of information encoded within the ground-truth concept annotations. Thus, concepts with higher base rates are more likely to be used within the explanation. For **UU** and **U** formulations, this is not the case, since we use either the learned scores for the concepts (either $h_{\text{conc}} \circ f(x)$ or a probabilistic version of it), and these continuous vectors contain information regardless of the base rates of the concepts. Next, the *size* of the concept can influence its *learnability*: larger concepts can be easier for a model to learn, thus, these concepts are more likely to be used to learn a scene class. However, for the **UU** and **U** formulations, we note that the concept encodings could include other information within it (potentially even additional unlabelled concepts). Thus, the selected concepts might be the ones that are themselves less learnable.

4.2. Comparison to prior work

Finally, we consider prior works that generate concept-based explanations and analyze them within our framework.

We find that we are able to express all concept-based explanations [4, 8, 12, 31, 16, 22] in our framework (see supp. mat. for more details). For methods whose optimizations are slightly from ours [4, 31, 22], we also run the closest form of our optimization along with their method, and compare the results produced.

NetDissect [4]. Rather than explaining the full output of the network $F(x) \in \mathbb{R}^D$, NetDissect explains $F(x) \in \mathbb{R}$ for each neuron. Furthermore, NetDissect correlates the neuron’s output with the pixel-level *segmentation* of each concept so the formulation changes slightly to accommodate predicting concepts at an image-level to a pixel-level. Generally, this can be achieved with $\lambda_1 = 0$ and changing L_{align} to denote how well aligned an individual neuron’s output is to concept segmentations. Within our optimization, we set $\lambda_1 = 0$ and optimize h_{conc} to find the best semantic concept for each neuron. While this is different to the segmentation intersection over union (IOU) score that NetDissect uses, we still identify similar explanations (Tab. 3).

Concretely, as in NetDissect, we set f to the output of the final convolutional layer in the ResNet18 [10], which outputs a 7×7 feature map for each neuron. ADE20k [32, 33] is labelled with segmentation masks. Thus, for each of the 49 regions, we are able to identify the most common object (or object part) and use this as a coarse segmentation map. We compute alignment using normalized AP [11] between the coarse segmentation map and the output of the neuron. Other implementation details remain the same as before.

Net2Vec [8] and TCAV [12]. Similar to NetDissect [4], these methods aim to explain the output of an intermediate layer. Here, h_{conc} is a linear function that finds the best mapping from the feature space f for each concept, and our optimization is exactly the same as that of these methods.

IBD [31]. Here, the method attempts to explain the logits of the model. It assumes that both h_{conc} and h_{pred} are linear functions, and that the feature space f is the output of the final convolutional layer. IBD optimizes Eq. (7), and thus is a (**UU**, **FF**) method. They optimize this equation by first computing h_{conc} as a sequence of orthogonal vectors (called an “interpretable basis”). They then express the model output as a linear combination of these basis vectors, with each weight being positive. They also limit the number of concepts per target class. This can be modelled by optimizing S and h_{pred} per target class. Here, the main difference is that IBD adds a non-negative constraint to the coefficients in h_{pred} . This constraint appears to significantly affect concept selection, such that the set of concepts selected using the constraint vs. without it do not overlap in general. (results in the supp. mat.)

Concept Bottleneck models [16, 18, 20, 6]. Unlike the other methods, Concept Bottleneck (CB) models are “interpretable-by-design”. These models are learned as a

neuron	NetDissect [4]		UFO (top 3 concepts)					
	top concept	IOU	concept-1	nAP-1	concept-2	nAP-2	concept-3	nAP-3
454	car	0.2184	car	94.4	saddle	94.0	van	92.2
193	skyscraper	0.2055	water tower	99.2	skyscraper	96.8	control tower	95.3
445	car	0.2014	saddle	99.0	car	96.1	teapot	95.8
446	pool table	0.1928	pool table	97.8	table tennis	96.6	arcade machine	96.2
500	sofa	0.1558	sofa	94.2	bed	93.0	armchair	91.4
46	house	0.1549	house	96.1	pavilion	94.8	windmill	92.0
341	sea	0.1531	sea	98.0	lighthouse	93.0	ship	91.1
43	bed	0.1509	bed	96.9	pillow	96.8	eiderdown	96.0
484	water	0.1496	water	92.0	sea	91.3	river	90.3
329	pool table	0.1474	pool table	97.6	table tennis	97.0	court	94.8

Table 3. **Comparison with NetDissect.** We show results for the 10 neurons that have the highest IOU scores with a concept in NetDissect [4] alongside the top 3 concepts that best explain those units (i.e., highest normalized AP [nAP]) using our formulation. Despite slight differences in the optimizations, we see that the concepts correspond well: the top concept from our explanation matches that of NetDissect for most units. Concepts from our optimization that match the top concept from NetDissect are **bolded**.

composition of two functions, one that maps images to concepts and another that maps concepts to the final output. We focus on one, the concept bottleneck model [16], but others are similar. In our framework, this is an (U, FF) method, i.e, it optimizes Eq. (6)⁴, where h_{conc} is the identity function and h_{pred} is g itself. All concepts are allowed to be used within the explanation. However, the explanations generated can be hard to understand given the large number of concepts used, and the continuous encoding of the concepts. Removing the constraint of the number of concepts selected make the optimizations between Concept Bottleneck and the (U, FF) identical, and hence, we do not run experiments.

ELUDE [22]. In this work, the authors ignore the mapping from the features to the concepts entirely, with $\lambda_2 = 0$. They use the least faithful (F) and most understandable (UUU) definition and optimize Eq. (11). Rather than pre-deciding K , they add a regularization constraint when optimizing to use fewer concepts. The main difference between the optimization (UUU, F) and ELUDE is in its L1 penalty. ELUDE enforces that the number of concepts used per target class is minimized using an L1 penalty (the total number of concepts used might be large), whereas we use a grouped L1 penalty to minimize the total number of concepts used.

Thus, we optimize Eq. (11) per target class. For each coarse-grain scene group, we compare the concepts selected using this modified formulation (using $K = 8$ concepts) to the ones selected by ELUDE and report the number of common concepts between these two explanations in Fig. 4 For a given class, we find that the number of common concepts increases with its the base rate of the class (i.e, if sufficient positive examples of the class exist, the concepts used by ELUDE and our formulation align well (Fig. 4).

⁴Koh et al. [16] also try adding a sigmoid layer after predicting concepts (i.e, optimizing Eq. 7), but found a significant drop in model accuracy.

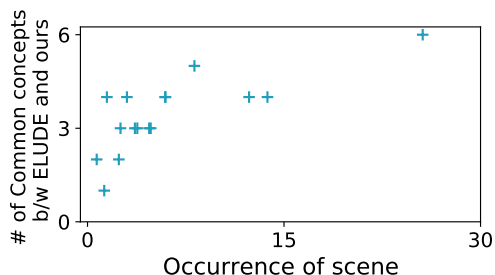


Figure 4. **Comparison with ELUDE.** The least faithful, most understandable (UUU, F) formulation of UFO produces explanations similar to ELUDE [22], particularly for scene classes that are frequent in the probe dataset. For each coarse-grained scene group, we plot the base rate of the scene class within ADE20k and the number of concepts shared between the explanations.

5. Conclusion

We present a unified method (UFO) that formalizes faithfulness and understandability as mathematical objectives and encapsulates existing concept-based explanation methods. We show how tuning the knobs of these two objectives affects how much of the model’s behavior is explained as well as how and why concept selection varies based on these objectives (e.g., more understandable explanations select concepts that are larger and more learnable). We also compare outputs of UFO to existing methods, and show that it is very similar to NetDissect and similar to ELUDE for well represented within the probe dataset. Our work clearly synthesizes how existing works compare to one another for the first time and provides a useful paradigm through which future methods can be developed and described.

Acknowledgements. We thank Angelina Wang, Byron Zhang, Rohan Jinturkar and rest of the Princeton Visual AI Lab members (especially Nicole Meister) who provided

helpful feedback on our work. This material is based upon work partially supported by the National Science Foundation under Grants No. 1763642, 2145198 and 2112562. Any opinions, findings, and conclusions or recommendations expressed in this material are those of the author(s) and do not necessarily reflect the views of the National Science Foundation. We also acknowledge support from the Princeton SEAS Howard B. Wentz, Jr. Junior Faculty Award to OR, Princeton SEAS Project X Fund to RF and OR, Open Philanthropy Grant to RF, and NSF Graduate Research Fellowship to SK.

References

- [1] Julius Adebayo, Justin Gilmer, Michael Muelly, Ian Goodfellow, Moritz Hardt, and Been Kim. Sanity checks for saliency maps. In *NeurIPS*, 2018.
- [2] Julius Adebayo, Michael Muelly, Harold Abelson, and Been Kim. Post hoc explanations may be ineffective for detecting unknown spurious correlation. In *ICLR*, 2022.
- [3] Julius Adebayo, Michael Muelly, Ilaria Lliccardi, and Been Kim. Debugging tests for model explanations. In *NeurIPS*, 2020.
- [4] David Bau, Bolei Zhou, Aditya Khosla, Aude Oliva, and Antonio Torralba. Network dissection: Quantifying interpretability of deep visual representations. In *CVPR*, 2017.
- [5] Aditya Chattopadhyay, Anirban Sarkar, Prantik Howlader, and Vineeth N Balasubramanian. Grad-CAM++: Generalized gradient-based visual explanations for deep convolutional networks. In *WACV*, 2018.
- [6] Abhimanyu Dubey, Filip Radenovic, and Dhruv Mahajan. Scalable interpretability via polynomials. In *NeurIPS*, 2022.
- [7] Ruth Fong, Mandela Patrick, and Andrea Vedaldi. Understanding deep networks via extremal perturbations and smooth masks. In *ICCV*, 2019.
- [8] Ruth Fong and Andrea Vedaldi. Net2vec: Quantifying and explaining how concepts are encoded by filters in deep neural networks. In *CVPR*, 2018.
- [9] Tessa Han, Suraj Srinivas, and Himabindu Lakkaraju. Which explanation should I choose? A function approximation perspective to characterizing post hoc explanations. *arXiv:2206.01254*, 2022.
- [10] Kaiming He, Xiangyu Zhang, Shaoqing Ren, and Jian Sun. Deep residual learning for image recognition. In *CVPR*, 2016.
- [11] Derek Hoiem, Yodsawalai Chodpathumwan, and Qieyun Dai. Diagnosing error in object detectors. In *ECCV*. Springer, 2012.
- [12] Been Kim, Martin Wattenberg, Justin Gilmer, Carrie Cai, James Wexler, Fernanda Viegas, and Rory Sayres. Interpretability beyond feature attribution: Quantitative testing with concept activation vectors (TCAV). In *ICML*, 2018.
- [13] Sunnie S. Y. Kim, Nicole Meister, Vikram V. Ramaswamy, Ruth Fong, and Olga Russakovsky. HIVE: Evaluating the human interpretability of visual explanations. In *ECCV*, 2022.
- [14] Sunnie S. Y. Kim, Elizabeth Anne Watkins, Olga Russakovsky, Ruth Fong, and Andrés Monroy-Hernández. “Help me help the AI”: Understanding how explainability can support human-AI interaction. In *CHI*, 2023.
- [15] Diederik P Kingma and Jimmy Ba. Adam: A method for stochastic optimization. In *ICLR*, 2015.
- [16] Pang Wei Koh, Thao Nguyen, Yew Siang Tang, Stephen Mussmann, Emma Pierson, Been Kim, and Percy Liang. Concept bottleneck models. In *ICML*, 2020.
- [17] Satyapriya Krishna, Tessa Han, Alex Gu, Javin Pombra, Shahin Jabbari, Steven Wu, and Himabindu Lakkaraju. The disagreement problem in explainable machine learning: A practitioner’s perspective. *arXiv:2202.01602*, 2022.
- [18] Diego Marcos, Ruth Fong, Sylvain Lobry, Rémi Flamary, Nicolas Courty, and Devis Tuia. Contextual semantic interpretability. In *ACCV*, 2020.
- [19] Vitali Petsiuk, Abir Das, and Kate Saenko. RISE: Randomized input sampling for explanation of black-box models. In *BMVC*, 2018.
- [20] Filip Radenovic, Abhimanyu Dubey, and Dhruv Mahajan. Neural basis models for interpretability. In *NeurIPS*, 2022.
- [21] Vikram V. Ramaswamy, Sunnie S. Y. Kim, Ruth Fong, and Olga Russakovsky. Overlooked factors in concept-based explanations: Dataset choice, concept salience, and human capability. In *CVPR*, 2023.
- [22] Vikram V. Ramaswamy, Sunnie S. Y. Kim, Nicole Meister, Ruth Fong, and Olga Russakovsky. ELUDE: Generating interpretable explanations via a decomposition into labelled and unlabelled features. *arXiv:2206.07690*, 2022.
- [23] Ramprasaath R Selvaraju, Michael Cogswell, Abhishek Das, Ramakrishna Vedantam, Devi Parikh, and Dhruv Batra. Grad-CAM: Visual explanations from deep networks via gradient-based localization. In *ICCV*, 2017.
- [24] Karen Simonyan, Andrea Vedaldi, and Andrew Zisserman. Deep inside convolutional networks: Visualising image classification models and saliency maps. *arXiv:1312.6034*, 2013.
- [25] Kacper Sokol and Peter Flach. Explainability fact sheets: A framework for systematic assessment of explainable approaches. In *FAccT*, 2020.
- [26] Ming Yuan and Yi Lin. Model selection and estimation in regression with grouped variables. *J. R. Stat. Soc.*, 2006.
- [27] Matthew D Zeiler and Rob Fergus. Visualizing and understanding convolutional networks. In *ECCV*, 2014.
- [28] Jianming Zhang, Sarah Adel Bargal, Zhe Lin, Jonathan Brandt, Xiaohui Shen, and Stan Sclaroff. Top-down neural attention by excitation backprop. *IJCV*, 2018.
- [29] Bolei Zhou, Aditya Khosla, Agata Lapedriza, Aude Oliva, and Antonio Torralba. Learning deep features for discriminative localization. In *CVPR*, 2016.
- [30] Bolei Zhou, Agata Lapedriza, Aditya Khosla, Aude Oliva, and Antonio Torralba. Places: A 10 million image database for scene recognition. *TPAMI*, 40, 2017.
- [31] Bolei Zhou, Yiyou Sun, David Bau, and Antonio Torralba. Interpretable basis decomposition for visual explanation. In *ECCV*, 2018.
- [32] Bolei Zhou, Hang Zhao, Xavier Puig, Sanja Fidler, Adela Barriuso, and Antonio Torralba. Scene parsing through ADE20k dataset. In *CVPR*, 2017.

[33] Bolei Zhou, Hang Zhao, Xavier Puig, Tete Xiao, Sanja Fidler, Adela Barriuso, and Antonio Torralba. Semantic understanding of scenes through the ADE20k dataset. *IJCV*, 2019.

In this appendix, we provide more details about our method, as well as some additional results.

A. Additional details about comparisons with prior work

Here we provide more details about the different methods, and how they can be thought of within our framework.

Net2Vec and TCAV. For Net2Vec [8] and TCAV [12], the authors align the feature space with concepts, without considering the final output. This can be achieved with $\lambda_1 = 0$. The authors allow the features f to be any layer within the trained model M , and learn h_{conc} as a series of individual indicator functions to the concepts for each neuron in f or as a linear combination of the different neurons in f , i.e. $h_{\text{conc}}: \mathbb{R}^n \rightarrow \mathbb{R}^C$, where n is the number of neurons in a layer of the CNN and C is the number of concepts. The authors allow the selection function S to select all the C concepts, i.e. $K = C$. Thus, these works optimize L_{align} :

$$L_{\text{align}}^{\text{Net2Vec, TCAV}} = \sum_{j \in \{1, 2, \dots, C\}} \sum_{x \in X} CE(A(x)_j, (h_{\text{conc}} \circ f(x))_j) \quad (13)$$

Net2Vec also considers aligning individual neurons with concepts. This can be achieved by forcing h_{conc} to be an indicator function: each neuron is aligned with exactly one concept.

NetDissect. NetDissect [4] uses a slightly different framework compared to ours, however, we show that by rewriting L_{align} , we can consider NetDissect within our framework. We first rewrite NetDissect using the following notation.

- Suppose $A_{\text{seg}}: X \rightarrow \mathbb{R}^{C \times H \times W}$ is the segmentation map for C concepts.
- $f: \mathcal{X} \rightarrow \mathbb{R}^{n \times H' \times W'}$ is the feature space.
- $t: \mathbb{R}^{n \times H' \times W'} \rightarrow \{0, 1\}^{D \times H \times W}$. This is an upsampling and thresholding function: first, the vector is bilinearly upsampled to size $H \times W$ for each neuron, and thresholded such that only the top 0.5% for a neuron is activated.

Now, for each neuron $i \in \{1, 2, \dots, n\}$, they compute the concept j that maximizes

$$\text{IOU}_i := \arg \max_{j \in \{1, 2, \dots, C\}} \left(\frac{\sum_{x \in X} ((A_{\text{seg}}(x))_j \cap (t \circ f(x))_i)}{\sum_{x \in X} ((A_{\text{seg}}(x))_j \cup (t \circ f(x))_i)} \right) \quad (14)$$

In order to consider NetDissect within our framework, we can rewrite L_{align} as follows. We first consider f_i at a single neuron i , i.e. $f_i: \mathcal{X} \rightarrow \mathbb{R}^{H' \times W'}$. Then, rather than using $\sum_x CE(A(x), h_{\text{conc}} \circ f(x))$, we can express L_{align} in terms of Eq. (14), with $|S| = 1$:

$$L_{\text{align}} = - \sum_{j \in \{1, 2, \dots, C\}} \mathbb{1}_S \circ \text{IOU}_j \quad (15)$$

IBD. For IBD [31], h_{conc} is a linear combination of the activations of each neuron and h_{pred} is a linear combination of the outputs of h_{conc} , very similar to our **sf, su** framework. The main difference is in an additional constraint imposed on h_{pred} : that the coefficients are all non-negative, and each target class is allowed to use exactly K concepts (but these do not need to be the same across target classes). Thus, for IBD, L_{mimic} can be written as:

$$\forall i \in \{1, 2, \dots, D\} \\ (L_{\text{mimic}}^{\text{IBD}})_i = \sum_{x \in X} \|(g \circ f(x))_i - h_{\text{pred}}^i \circ \mathbb{1}_{S_i} \circ p \circ h_{\text{conc}} \circ f(x)\| \quad (16)$$

such that

$$h_{\text{pred}}^i(x) = W_i^T f(x) \\ W_{i,k} \geq 0 \quad \forall k \in \{1, 2, \dots, n\}$$

As mentioned in the main text Section 5.2, the non-negative constraint changes the concepts chosen: examples of concepts chosen are in table 4

B. More results

In this section, we give more details about our experiment set up and highlight additional results.

Experimental setup. We use a greedy method to select uncorrelated concepts, using Pearson’s correlation coefficient. For each understandability setting, we compute the correlation coefficient between all pairs of concepts (using either the base rates or the learned concept vector). Next, we compute the 90% percentile correlation coefficient and set that as a threshold. We add each concept to the list of chosen concepts if it is not more correlated than the threshold with any of the previously chosen concepts.

When choosing the values of λ_1 and λ_2 , we fix λ_1 to 1, and pick λ_2 from $\{1.0, 0.5, 0.1, 0.05, 0.01, 0.005\}$ that best explains the model on the validation set.

Concepts for coarse grained scenes. We first report the concepts chosen across the 6 faithfulness-understandability settings described in the main text. Similar to the fine-grained model, we see that the attributes chosen vary based on the setting (Tab. 5).

scene	IBD	UFO(Ours)
attic	heater, basket, stairway, breads, magazine, television camera, drum	backpack, grandstand, coffee maker, pitcher, microwave, sand, door, sculpture
bathroom	screen door, village, water tower, tray, candelabrum, stands, drinking glass	grandstand, backpack, crt screen, bench, microwave, double door, sculpture, work surface
bedchamber	headboard, pillow, shade, vault, eiderdown, water tower, tent	coffee maker, pitcher, spotlight, microwave, cabinet, door, sky, sculpture
bedroom	headboard, pillow, eiderdown, shade, lower sash, shower, shirt	grandstand, coffee maker, doorframe, ladder, sculpture, spotlight, work surface, clock
conference-room	bulletin board, wineglass, trouser, escalator, mouse, button panel, mouse pad	grandstand, platform, counter, pitcher, microwave, ladder, floor, desk
crosswalk	vineyard, traffic light, autobus, chain wheel, trailer, skylight, cockpit	coffee maker, grandstand, land, platform, crt screen, backpack, doorframe, television
dining-room	chandelier, candelabrum, back pillow, skirt, carpet, cart, grand piano	coffee maker, pitcher, platform, chest, windowpane, road, door, table
downtown	skyscraper, paper towel, gas station, candelabrum, place mat, slot machine, crosswalk	grandstand, land, pitcher, platform, crt screen, television, sky, sofa
highway	catwalk, autobus, document, book stand, dashboard, slats, corner pocket	coffee maker, platform, plant, flag, sky, lamp, door, table
hotel-room	bed, tracks, candlestick, cushion, seat cushion, capital, candle	land, microwave, spotlight, cabinet, sculpture, dishwasher, clock, work surface
kitchen	stove, refrigerator, tray, kitchen island, container, screen door, microwave	grandstand, coffee maker, backpack, crt screen, pitcher, doorframe, cap, faucet
living-room	post, cushion, riser, fireplace, monitoring device, sconce, bumper	pitcher, doorframe, counter, spotlight, windowpane, cabinet, door, table
parking-garage/outdoor	paper towel, crane, windows, notebook, steam shovel, gym shoe, television	coffee maker, grandstand, land, backpack, platform, crt screen, doorframe, television
recreation-room	pool table, court, microwave, table football, slot machine, wire, grand piano	grandstand, land, chest, counter, spotlight, floor, windowpane, sky
residential-neighborhood	sill, balloon, trailer, metal shutters, flowerpot, switch, synthesizer	coffee maker, faucet, land, platform, doorframe, sculpture, dishwasher, floor
skyscraper	skyscraper, display board, workbench, manhole, paw, lighthouse, gas station	coffee maker, land, pitcher, television, sky, sofa, lamp, spotlight
street	slats, roundabout, crosswalk, beak, arcades, bus, parking	coffee maker, land, faucet, platform, crt screen, microwave, doorframe, television
television-room	seat base, brick, sash, inside arm, gravel, water wheel, pantry	pitcher, chest, cap, microwave, spotlight, counter, desk, door
waiting-room	armchair, sconce, shoe, console table, back pillow, canvas, dishrag	pitcher, chest, counter, spotlight, sky, doorframe, sofa, table
youth-hostel	sweater, towel, equipment, kettle, wardrobe, vent, partition	grandstand, doorframe, ladder, microwave, spotlight, sculpture, work surface, flag

Table 4. **Concepts chosen by IBD [31] versus that chosen by our method.** We see that the non-negative constraint added by IBD changes the concepts chosen by quite a lot.

		most understandable (UUU)	somewhat understandable (UU)	least understandable (U)
shopping-dining	FF	<i>bed</i> , bulletin board, <i>sky</i>	cap , <i>footbridge</i> , baby buggy	faucet , <i>land</i> , cap
	F	<i>grandstand</i> , <i>pillow</i> , <i>bird</i>	<i>table tennis</i> , cap , <i>loudspeaker</i>	faucet , pitcher, counter
workplace	FF	<i>sky</i> , floor, desk	dog , <i>footbridge</i> , baby buggy	platform, <i>bread</i> , <i>jar</i>
	F	<i>sky</i> , <i>bed</i> , <i>tree</i>	baby buggy , dog , <i>lake</i>	paper, bulletin board, runway
home-hotel	FF	<i>bed</i> , towel, floor	<i>footbridge</i> , <i>cap</i> , <i>railroad train</i>	table tennis, blind , bread
	F	<i>grandstand</i> , <i>road</i> , <i>bird</i>	<i>bulletin board</i> , <i>text</i> , <i>footbridge</i>	blind , faucet, <i>paper</i>
indoor-transport	FF	floor, <i>tree</i> , work surface	table tennis , railroad train , cap	clock , cap , railroad train
	F	<i>grandstand</i> , <i>dog</i> , <i>umbrella</i>	table tennis , cap , <i>lake</i>	backpack, clock , runway
indoor-cultural	FF	<i>sky</i> , work surface , desk	<i>lake</i> , <i>footbridge</i> , dog	sculpture, <i>trunk</i> , runway
	F	work surface , <i>towel</i> , central reservation	<i>land</i> , <i>microwave</i> , <i>exhaust hood</i>	paper, runway , <i>television</i>
water, ice, snow	FF	lake , mountain, <i>floor</i>	lake , <i>footbridge</i> , cap	land , backpack, refrigerator
	F	<i>grandstand</i> , <i>door</i> , <i>scaffolding</i>	horse , lake , <i>text</i>	counter, land , horse
mountains, hills, desert	FF	mountain , <i>sky</i> , <i>building</i>	<i>lake</i> , cap, land	backpack, land , mountain
	F	<i>bird</i> , <i>windowpane</i> , <i>grandstand</i>	<i>footbridge</i> , <i>text</i> , <i>signboard</i>	<i>flag</i> , land , mountain
forest, field, jungle	FF	<i>tree</i> , <i>building</i> , <i>road</i>	<i>footbridge</i> , trunk , horse	horse , trunk , <i>ladder</i>
	F	<i>central reservation</i> , bulletin board , spotlight	trunk , horse , spotlight	bulletin board , horse , <i>forecourt</i>
outdoor-transport	FF	<i>road</i> , <i>sky</i> , <i>building</i>	<i>lake</i> , cap , <i>footbridge</i>	runway , bulletin board, ladder
	F	<i>desk</i> , <i>rack</i> , <i>towel</i>	<i>lake</i> , cap , horse	runway , pitcher, horse
cultural-historic	FF	<i>building</i> , lake , <i>sky</i>	baby buggy, lake , trunk	forecourt, trunk , <i>table tennis</i>
	F	<i>fluorescent</i> , <i>cabinet</i> , <i>bed</i>	lake , <i>horse</i> , <i>railroad train</i>	<i>pitcher</i> , <i>blind</i> , <i>runway</i>
sports fields, parks	FF	<i>grandstand</i> , <i>desk</i> , <i>tree</i>	baby buggy , <i>lake</i> , <i>cap</i>	baby buggy , net , <i>paper</i>
	F	<i>scaffolding</i> , <i>air conditioner</i> , <i>curtain</i>	baby buggy , <i>telephone booth</i> , <i>lake</i>	net , table, <i>double door</i>
cabins, gardens, farms	FF	<i>tree</i> , plant, <i>bulletin board</i>	table tennis , <i>cap</i> , dog	table tennis , <i>blind</i> , <i>backpack</i>
	F	<i>bird</i> , <i>spotlight</i> , <i>scaffolding</i>	<i>land</i> , <i>lake</i> , <i>railroad train</i>	bread, counter, <i>poster</i>
comm-buildings/towns	FF	<i>building</i> , grandstand , <i>road</i>	telephone booth, trunk, land	forecourt , platform, <i>net</i>
	F	grandstand , <i>desk</i> , <i>piano</i>	land , <i>horse</i> , <i>lake</i>	forecourt , poster, <i>flag</i>

Table 5. **Selected concepts vary based on faithfulness-understandability setting.** Similar to the main text Tab. 2., we examine the concepts chosen for each scene group across 6 settings ($\{\text{UUU}, \text{UU}, \text{U}\} \times \{\text{FF}, \text{F}\}$). We report the 3 concepts with highest absolute weights within the explanation. Common concepts are **bolded**, *Red* denotes that the coefficient is negative, whereas *blue* denotes that the coefficient is positive. We note that the concepts highlighted are typically not shared among different explanations